Investigation of the Microstructure and Mechanical Properties of S355JR – S700MC Steels Welded by GMAW

Fatma Nur ŞAHİN
Necmettin Erbakan University

Hakan GÖKMEŞE
Necmettin Erbakan University

Şaban BÜLBÜL
Necmettin Erbakan University

To Cite This Chapter:
Şahin, F. N., Gökmeşe, H., & Bülbül, Ş. (2025). Investigation of the microstructure and mechanical properties of S355JR–S700MC steels welded by GMAW. In H. Gökmeşe, Ş. Bülbül, & Y. Uzun (Eds.), Current studies in basic sciences: *Innovative approaches in materials science and applications* (pp. 47–64). ISRES Book Series. ISRES Publishing.

Introduction

Following the Stone Age, the discovery of metals led to the development of processing methods. For the people of that era, who subsisted on hunting, metals used particularly in weapon production gained significant importance. After the discovery of gold, copper, silver, lead, and tin, iron was discovered around 1500 BC. Subsequently, many different types of metals, such as chromium, aluminium, and nickel, were discovered. As history progressed, the smelting of iron was discovered and used in the manufacture of tools and weapons. In the Bronze Age, the foundations of alloying were laid, and it was discovered that two different metals could be mixed to obtain a stronger metal.

With the technology that developed after the Industrial Revolution, steel was added to iron, which had been used since ancient times, forming the basis of industry. With this development, production techniques also changed. Welding, which enables two materials to be joined together in a strong manner, has also gained great importance in heavy industry. Known as blacksmithing in ancient times, this method has been developed using different techniques with the discovery of steel and other materials.

Welding, one of the most important production methods used in industry, involves melting and joining multiple materials using different techniques. Starting with joining by hammer blows, welded manufacturing was further developed with the discovery of sources such as oxygen and electricity. Applications were made using oxyacetylene, electric arc welding, TIG, GMAW (MIG and MAG welding) methods, respectively. With advancing technology, many different welding techniques have been developed, such as submerged arc welding, resistance welding, and laser welding.

Due to the widespread use of steel as a raw material in industry, MIG/MAG welding applications are particularly prevalent. In many sectors, such as automotive and construction, the MAG welding method is preferred due to its cost and good welded joints in terms of mechanical and chemical properties. Since the effect of shielding gas is very high in this welding method, it has been the subject of many scientific studies. Argon-rich carbon dioxide and oxygen additives are particularly preferred for their high-quality weld seam, economy, and availability.

In addition to structural steels such as S235 and S355, which have a wide range of uses, the use of high-strength SSAB brand Strenx lightweight structural steels has also become widespread. They are particularly preferred in the automotive industry because they can carry more load than other steels of the same weight. Companies that choose these steels due to the expectation that load-bearing transport vehicles in Europe should be lighter are also achieving significant financial gains in exports.

In the automotive sector, the welded combination of S700MC and S355JR steel is a common application in trailer and body manufacturing. Deformations in the material are likely when incorrect application techniques are used. Experimental research was conducted in this thesis to understand the weld structure and mechanical properties of these products, which carry very high tonnages.

In this study, S355JR structural steel and S700MC fine-grained structural steel, which are widely used in industry, were welded using the MAG welding method, using SG2 welding wire with a diameter of 1.2 mm and protective gases of 86%Ar+12%CO_2+2%O_2 and 93%Ar+5%CO_2+2%O_2. The welded areas of the steels, the grain structure changes in the HAZ and parent metal, and the mechanical properties were examined.

Welding Methods

Welding is defined as metal or plastic welding, depending on the type of material to be applied. If heat input is involved in the applied method, it is fusion welding, and in some applications of this method, a filler metal is used to join the two materials. If welding is performed under pressure, it is called pressure welding. In pressure welding, the material is heated and joined under pressure in the area without the use of any filler metal.

When classified according to the purpose of welding, it is defined as joining and filling welding; it is classified according to the type of material as metal and plastic welding. The method used to join multiple materials into an inseparable whole is called joining welding. while the method used to fill a gap in a part or to enlarge a part is called filling welding (Anık, 1991).

Gas Metal Arc Welding (GMAW)

In gas metal arc welding, which is performed with a consumable electrode, a shielding gas is used to protect the weld pool from the adverse effects of the air. If the welding gas used is inert, it is called MIG (Metal Inert Gas) welding, and if it is active, it is called MAG (Metal Active Gas) welding (Koç, 2009). During welding, the welding gas passes through the welding torch over the wire and covers the weld pool. In this welding method, the arc is established between the welding wire and the contact nozzle and is transferred to the workpiece via the wire.

Argon and helium gases are commonly used as inert gases in MIG welding. In MAG welding, mixtures of gases consisting of carbon dioxide or inert gases mixed with carbon dioxide in specific proportions are used as active gases. In this method, depending on the intended use, electrodes can be made into cored wires by feeding them with various minerals to obtain a more efficient and higher-quality weld. The equipment and hardware used in MIG and MAG welding are identical; only the gas and electrode used differ. MIG welding is a suitable method for unalloyed and low-alloy steels. MAG welding can also be used for welding aluminium, copper, nickel, and titanium alloys (Toprak Şenol, 2020).

Figure 1

Principle of GMAW (Antonini, 2014)

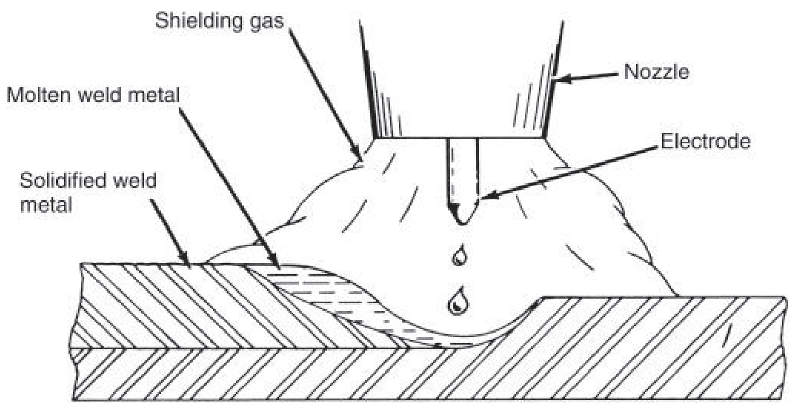

Principle of GMAW

In the GMAW method, a continuously fed consumable electrode is used together with a shielding gas. In semi-automatic welding machines, the free wire length and electrical characteristics of the arc set by the welder are automatically determined; the welder only controls the position of the welding torch and the feed rate.

The arc, which is created by the contact of the wire fed through the torch with the part, passes through an ionized gas with the electric current and melts with the heat generated. The energy generated by the movement of electrons travelling rapidly from the cathode to the anode releases heat, and the material in the heated area begins to melt. Atoms that lose electrons become ionised and rapidly move towards the cathode. As a result, melting also occurs in that heated area. Melting continues in this manner continuously **(Figure 1)**. The metal and wire being welded melt with the heat created by this welding. The molten wire, protected by shielding gas, fills the weld pool, which is also protected by the gas, as filler metal. After the arc is extinguished in the fusion zone, the weld metal solidifies (Şık, 2002).

As shown in **Figure 2**, in GMAW, the transfer of metal droplets to the weld metal occurs through three different mechanisms:

- Short-circuit transfer
- Large droplet transfer (Globular Transfer)
- Spray transfer

The droplet transfer type varies depending on many parameters, such as the type of shielding gas, the properties of the welding wire, the free wire length, and the type and intensity of the welding current (Eryürek, Sevük, & Odabaş, 2007).

Figure 2

Droplet Transfer Mechanisms ('Morrow Welding', n.d.)

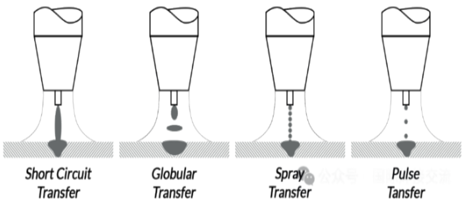

A short circuit transfer occurs in gas shielded welding performed at very low currents with low electrode diameters. Metal transfer to the workpiece does not occur in the arc gap; it only occurs when the electrode contacts the weld pool. In short-circuit transfer, the chemical composition of the shielding gas significantly affects the metal droplet diameter, arc characteristics, penetration into the workpiece, and short-circuit duration. Carbon dioxide provides deeper penetration than noble gases but causes more spatter. To achieve this balance, a mixture of carbon dioxide and argon is generally preferred. An argon-helium mixture also provides good penetration in metals other than iron. In large droplet transfer, the metal droplet diameter is larger than the electrode diameter. Large droplet transfer, where the type of shielding gas is not decisive, occurs at low welding currents with direct current and positive electrode polarity. It occurs at all welding currents when performed only with carbon dioxide and helium gases. In welds performed entirely with inert gas shielding, a globular transfer can be achieved at a current value slightly higher than the short circuit transfer current. Spray transfer can be achieved without spattering under argon gas shielding, with the electrode positively polarised in direct current, and when the current intensity is higher than the critical transition current value.

Metal transfer occurs when droplets smaller than the electrode diameter separate at a transfer rate of hundreds of droplets per second. The melting temperature and chemical composition of the shielding gas affect the transition current. Furthermore, the transition current is inversely proportional to the electrode diameter and free wire length. When spray transfer is performed under argon gas shielding, it can be used with almost all alloy metals (Eryürek et al., 2007).

GMAW Welding Equipment

The equipment used in gas shielded welding is divided into five main groups: the power unit, the shielding gas unit, the electrode feed unit, the welding torch, and the cable assembly **(Figure 3)**. Gas shielded arc welding equipment has a more complex structure than electric arc welding equipment (Küpeli, 2008).

Figure 3

GMAW Equipment (Stephanie Oostman, 2021)

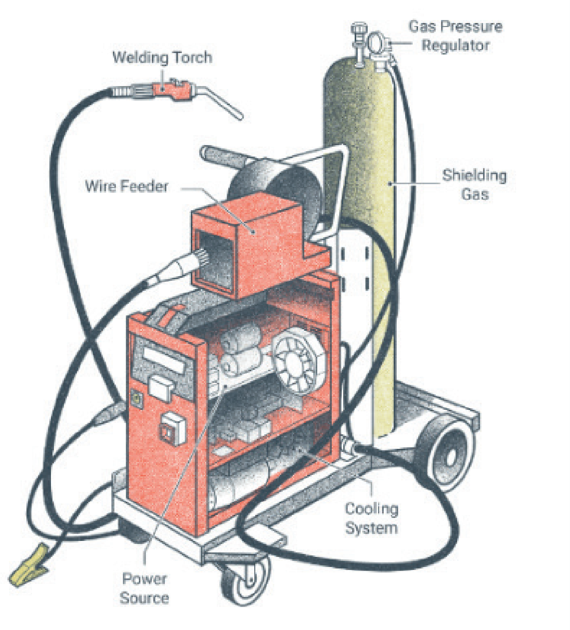

Electrodes (Welding Wires)

The wire-form electrodes used in GMAW are wound onto spools that meet specific standards (Durmuşoğlu, 2006). Electrodes are generally grouped according to their chemical composition and mechanical properties based on AWS standards, which are commonly used in the United States. According to German DIN standards, classification is based on wire diameter, surface tolerances and conditions, chemical composition, and application areas. The chemical compositions of electrodes used in the welding of steels commonly preferred in industry, according to DIN 8559 and TS 5618, are given in **Table 1**. Electrodes should be free of surface defects such as burrs, pits, and foreign matter that could impede their progression during welding; their surfaces should be completely smooth (Geçmen, 2006).

Table 1

Chemical Composition of Some Electrodes Used in Welding Steels (Geçmen, 2006)

Symbol	Mat. No	C	Si	Mn	P <	S <	Cu <	Impurity
SG 1	15112	0.07-.0.12	0.5-0.7	1.0-1.3	0.025	0.025	0.30	Cr 0.15 V 0.05 Zr+Ti 0.15 Al 0.02 Ni 0.15 Mo 0.15
SG 2	15125	0.07-0.14	0.7-1.0	1.3-1.6	0.025	0.025	0.30	
SG 3	15130	0.07-0.14	0.8-1.20	1.6-1.9	0.025	0.030	0.30	

The selection of consumable electrodes used in GMAW is crucial because the combination with the shielding gas affects the physical and chemical properties of the weld metal. The physical and mechanical properties of the weld metal and its chemical composition are selected according to the type of shielding gas. This selection is facilitated by knowing the effect of the components in the structure of the electrodes used in welding steels on the weld. These components are carbon, silicon, manganese, aluminium, titanium, zirconium, nickel, chromium, and molybdenum elements (Durmuşoğlu, 2006).

Shielding Gases

In MIG welding, inert gases such as argon and helium, which do not react, are used, while in MAG welding, active or active-inert gas mixtures such as carbon dioxide are used. The primary purpose of the shielding gases used in GMAW is to protect the weld pool and the area affected by heat from contamination and oxidation caused by the atmosphere. The molten metals in the weld pool absorb oxygen and nitrogen from the atmosphere, and these gases dissolve within the metal. The shielding gases can prevent these dissolved elements from forming compounds with the alloying elements in the metal and disrupting its chemical and physical structure, causing brittleness through the formation of pores and cracks. In addition, shielding gases affect welding characteristics such as welding speed, metal transfer mode, penetration and bead geometry, arc characteristics, and burn-off. The protective gases to be used are selected based on criteria such as part thickness, desired weld geometry, and mechanical properties, chemical composition of the base metal, cost and availability, and welding speed (Durmuşoğlu, 2006).

Weld Structure

A welded composite obtained by gas metal arc welding consists of the base metal, the weld metal formed by the mixture of the base metal and the filler metal, and the heat-affected zone (HAZ) **(Figure 4)**. In fusion arc welding, the mixture in the weld zone is complete and homogeneous. The amount of heat provided by the weld and the metal's ability to conduct this heat, as well as the weld speed, cause the width of the HAZ to vary (Karakoç, 2012).

Figure 4

Heat-affected Zone (HAZ) (Tukahirwa & Wandera, 2023)

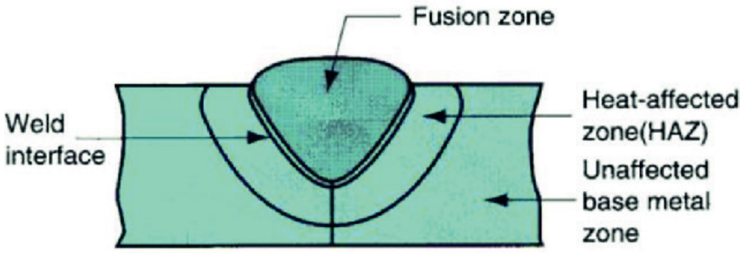

The weld metal is the region where the metal completely melts and then solidifies again during the welding process. The heat-affected zone (HAZ) is the non-melted region with different properties from the base metal due to the effect of the welding heat (Tukahirwa & Wandera, 2023).

Material and Methods

In this study, 4 mm thick S700MC and S355JR structural steels were used. Metal pieces measuring 200x200 mm were cut from sheet metal using plasma. The chemical compositions of S355JR2 are given in **Table 2,** and those of S700MC are given in **Table 3**.

Table 2

Chemical Composition of S355JR Structural Steel (%) (Dikeç, 2023)

C	Si	Mn	P	S	Al	Cu	Cr	N	Mo	Ni
0,186	0,13	1,426	0,011	0,008	0,036	0,121	0,042	0,0082	0,0002	0,059

Table 3

Chemical Composition of S700MC Structural Steel (%) (SSAB, 2023)

C	Si	Mn	P	S	Al	Nb	V	Ti
0,12	0,21	2,1	0,02	0,01	0,015	0,09	0,2	0,15

Of the steels whose mechanical properties are given in **Table 4,** S700MC steel has a stronger and harder structure than S355JR due to its fine-grained structure. Despite its high resistance under load, it is a very light steel. For this reason, it is widely preferred, especially in the automotive industry.

Table 4

Mechanical Properties of S355JR and S700MC Structural Steels (ChnÇelik, 2023)

Steel	Yield Strength (MPa)	Tensile Strength (MPa)	Elongation (%)
S355JR	355	470-630	22
S700MC	700	750-950	12

As O_2 gas was used during the cutting of the 200x200x4 mm metal parts, no further processing was required. Due to the low thickness of the parts to be butt welded, there was no need to open the weld joint. The parts were welded using 1.2 mm SG2 welding wire, which belongs to the ER70S-6 product group according to the AWS standard, under two different gas shields with composition ratios given in **Table 5**.

Table 5

Chemical Composition of HB205 ve HB212 (%)

	O_2	CO_2	Ar
HB 205	2	5	93
HB 212	2	12	86

The welding parameters were automatically set by the Kolarc M500 synergic welding machine by entering the material thickness of 4 mm, the type of welding gas, and the electrode diameter, and MAG welding was performed. Accordingly, the welding current intensity was set to approximately 200 A, the welding voltage to 20 V, and the wire feed speed to 7 m/min. The protective gas flow rate, one of the most important parameters determining the mechanical and chemical properties of the weld seam, was set to 12 m^3/s before starting the welding. The gas flow rate is theoretically calculated as 10 times the electrode diameter. In addition, to ensure full gas protection, the tip of the water-cooled torch is adjusted so that it does not lose its field of view and, when pulled perpendicular to the surface, is at most 20° from the surface.

In accordance with the standard ISO 5178:2019 Destructive tests on welds in metallic materials - Longitudinal tensile test on weld metal in fusion welded joints, two metal butt welds measuring 200x200 mm were welded on both sides using a thin material that was too thin to weld with the weld opening **(Figure 5a)**. Welding was performed in the PA (1G) position at a welding speed of 10 mm per second. Using a mixture of HB 205 and HB 212 gases, three samples each of 200x200 mm in size and 4 mm in thickness were welded under the same welding parameters: S355JR-S355JR, S355JR-S700MC, and S700MC-S700MC.

Figure 5
Welded Steel Samples

The samples were cut from the welded metal to approximately 50x90 mm as shown in **Figure 5b**. Due to the heat input, which would alter the properties of the material, the samples were cut to large dimensions. The flex-cut samples were prepared for water jet cutting for microstructure, microhardness, and XRD analysis. Small samples were cut to fit into the bakelite so that they would cover the base metal, HAZ, and weld zone of the material. Metal parts were placed in a moulding device together with two scales of Aka-Resin Acrylic bakelite powder. Samples processed in this device at 190 °C temperature and pressure for 15.5 minutes were ready for grinding.

For a clear image in microstructure examinations, the material's surface must be completely smooth, free of scratches and deformations. Therefore, the sample's surface was sanded using a sanding machine while submerged in water. The surface was processed with 400, 800, and 1200 grit sandpaper until it was completely smooth. Before each sanding, the surface of the sample was washed and cleaned with alcohol. As a final step, the felt was changed on the same machine, and the sample was polished dry. The polished samples were washed with soap, cleaned with alcohol, and dried.

Following metallographic studies conducted after the welding process, optical microscope examinations were performed to examine the microstructure of the test specimens. In particular, regarding the microstructural characterisation of the test specimens, the phase structures and their distributions, the examination of grains and grain boundaries, and the differences in the welding process in terms of HAZ and the base material were investigated.

In terms of welded manufacturing, phase transformation differences are important, particularly for the formation of the weld pool and HAZ region, within the scope of two different welding metals and welding parameter variables used. In this context, XRD analysis was performed to identify compounds that are likely to form depending on two different steel materials and welding parameters. The XRD analysis results were obtained using Cu-Kα radiation (λ= 1.544 Å) in the range of 10° $<2\theta<$70°, using a voltage of 40 kV and a current of 40 mA.

Microhardness measurements were performed to evaluate the hardness of the HAZ and weld metal of the test specimens as a result of the applied MAG welding method, depending on the difference in welding parameters. For these hardness measurements, studies were carried out under HV1 load on a Vickers-scale microhardness device. The microhardness measurement was automatically measured from the indentation mark left on the sample surface after pressing the diamond pyramid tip onto the sample surface for approximately 10 seconds with the load specified.

To perform the tensile test, the samples were designed in SolidWorks for cutting, as shown in **Figure 6a**, in accordance with the jaw dimensions of the tensile testing machine and the ISO 5178:2019 standard. In accordance with this standard, the laser method was preferred for cutting the specimens to be tested. The tensile bars were cut to the specified dimensions from each specimen, three pieces per specimen, as shown in **Figure 6b**, on a laser cutting bench programmed according to the design.

Figure 6

Tensile Test Samples

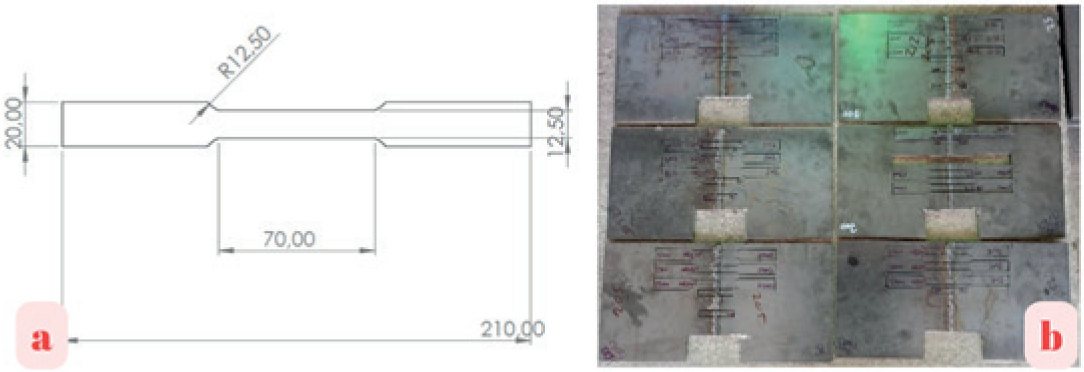

The test parameters were entered into the computer control programme compatible with the tensile testing machine, integrated with the ISO 6892-1 Metallic materials -Tensile testing- Part 1: Test method at ambient temperature standard. These parameters were set to a displacement speed of 5 mm/s and a loading speed of 0.2 kN/s, and the testing machine was started. Under these parameters, tensile tests were performed in triplicate for each sample, and the results obtained are given as average values.

Experimental Results

To describe the results obtained from the test specimens, the parts made of different steels welded under different gas shielding were named as follows:

- S355JR-S355JR steel sample welded with HB 20 gas S1
- S700MC-S700MC steel welded with HB 205 gas → S2
- S355JR-S700MC steel welded with HB 205 gas sample → S3

- S355JR-S355JR steel welded with HB 212 gas → S4
- S700MC-S700MC steel welded with HB 212 gas → S5
- S355JR-S700MC steel welded with HB 212 gas → → S6

The optical microstructure results obtained from the base metal, HAZ, and weld metal regions of S355JR and S700MC steel materials welded using the MAG welding method are shown in **Figure 7**, respectively.

Figure 7

Microstructural Analysis Results a)S1 b)S2 c)S3 d)S4 e)S5 f)S6

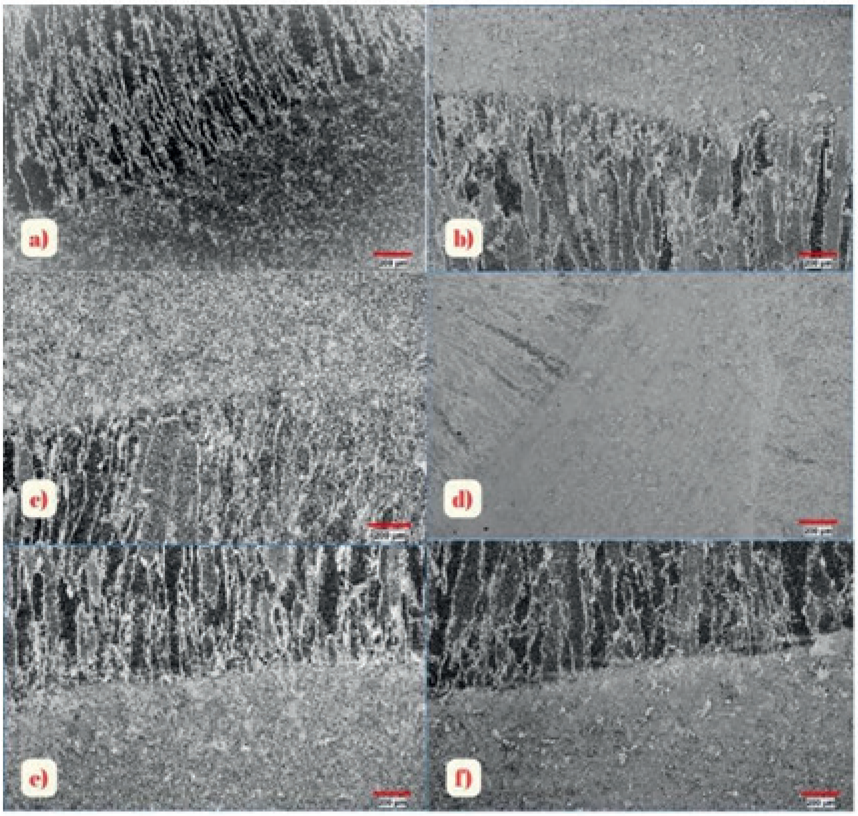

When examining the base metal of S355JR structural steel, it can be seen that the material consists of ferrite and pearlite phases. Moving to the HAZ and weld zone, this distinct structure is lost, and the grain size increases towards the weld metal. Coarse-grained dendritic arms are observed in the weld metal zone. Experimental studies in the literature indicate that grain growth in the weld metal zone is a result of increased heat input. Furthermore, it was observed that this heat causes grain orientation in the direction of flow (Kaya vd., 2020; Şık, 2007). Different composition ratios of the mixed gas did not create a significant difference in the microstructure. In S700MC steel, it was observed that the grain size increased as it progressed towards the HAZ and weld metal. As in S355JR steel, a dendritic structure was observed in the weld metal region. In these metals, the difference in welding gas also had no significant effect on the microstructure. A typical coarse-grained weld structure was also observed in the weld metal, which is the fusion zone of the S355JR and S700MC steel welds made using two different metals.

Grain coarsening from the base material towards the HAZ is a result of the welding heat input. Similarly, in the weld metal, coarse dendritic arms forming from the base material towards the centre of the weld metal also occur due to high heat input. In S355JR steel, a more ductile and soft structure has also formed due to slow cooling (Ayyıldız, 2022). In S700MC steel, despite the same cooling rates, it is considered that the original microstructure exhibits a martensitic structure. Consequently, following the welding process, no significant microstructural change was observed due to heat input, indicating that the martensitic and brittle structure was relatively preserved.

Figure 8

XRD Analysis Result

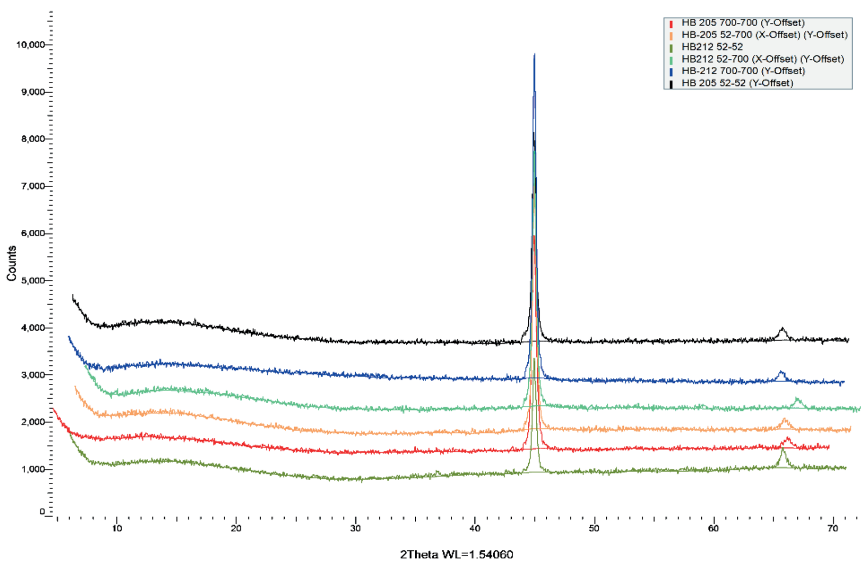

The results obtained from XRD analysis conducted to determine phase and phase transformations in the molten weld pool during the welding process of S355JR and S700MC steel materials using the MAG welding method, particularly under the influence of welding gas differences, were examined. The analysis revealed that the most intense fundamental peak in all materials was the iron (Fe) phase. Another intense but smaller peak can be seen to represent a small amount of iron phase. In materials of this type, the presence of austenitic alloying elements such as nickel and chromium in the weld metal indicates the presence of the iron phase (Górka & Stano, 2018). It is generally stated that in welded joints, the X-ray diffraction total intensity of iron and iron phases in terms of lattice plane can be limited to a range of 3-6% residual austenite content in the structure.

The combined XRD analysis results obtained in welded materials, depending on the HB 212 and HB 205 mixture gas difference, are given in **Figure 8**. Upon examination of the combined XRD analysis results, it can be stated that the microstructure of the base materials and welded joints consists of a ferrite phase. Another factor contributing to this situation is the use of the copper wavelength (1.544 Å) due to the XRD analysis device infrastructure used in the study. This is because the expected martensite structure has a smaller lattice parameter than a ferrite, and thus the martensite peaks cannot be displayed under the copper wavelength (Ekinci & Balalan, 2019).

When examining the microhardness results given in **Table 6**, considering that the hardness value is thought to be a maximum of 380 HV in the literature (Gür, 2022), it was determined that the obtained hardness values were below this value and consistent with the literature. The hardness values obtained in the base material after welded fabrication of S355JR materials were measured as 165-166 HV and 170-171 HV for HB 205 and HB 212 gas differences, respectively. Similarly, when the hardness values obtained in the S700MC base material were examined, they were measured as 305-310 HV and 304-301 HV for HB 205 and HB 212 gas differences, respectively. It can be stated that the hardness value of S700MC steel is higher than that of S355JR steel due to both the fine grain structure of the material and, in particular, the superior mechanical properties of this material and its high weldability (Çetin, 2019).

Looking at the microhardness measurement results according to the Vickers scale, an increase in hardness values is observed in S355JR steel due to high heat input. Conversely, in the more resistant S700 steel, a decrease in hardness is observed due to boron carbide precipitation at the austenite grain boundaries caused by its rolled structure (Eski, 2001).

When S355JR steel is welded with HB 212 mixed gas, the HAZ and weld metal are harder than when using HB 205 mixed gas. Based on this, it has been observed that HB 205 mixed gas gives better results when welding S355JR steel, as a 4 mm thick sheet metal is used. When looking at the weld of S700MC steel, in contrast to S355JR, higher hardness values were obtained when welding with HB 205 gas in the HAZ and weld metal. The increase in CO_2 content increased the heat input, causing a decrease in hardness due to the material's high hardness despite its low thickness. In this case, it was seen that the HB 205 mixture gas was more suitable for welding S700MC steels with each other and with S355JR steels.

Table 6
Microhardness Results of Welded Steel Samples

Sample Name	Base Metal	HAZ	Weld Metal	HAZ	Base Metal
S1	165	175	185	177	166
S4	170	208	239	201	171
S2	305	303	219	290	310
S5	304	298	198	261	301
S3	174	204	202	250	311
S6	177	222	209	223	312

Tensile tests were performed on three tensile bars from each sample, and the average values were taken to examine the yield and tensile strengths and the percentage elongation values. In addition to the test results obtained in the tensile test, the region where the tensile bar broke is also very important for interpreting the results. For the tensile specimens to be considered suitable, the fracture region must originate from the material itself, not the welded region (Özkan, 2019). When examining the samples obtained from the welds of S355JR steel with each other and with S700MC steel, a ductile fracture occurred appropriately on the S355JR material side. In the welds of S700MC steel with each other using both mixed gases, a fracture occurred inappropriately from the welded region. According to the data from the experimental studies, boron carbide precipitation causes a brittle structure at the grain boundaries, and the probability of intergranular fracture is high in this region where precipitation occurs (Eski, 2001). This has revealed the disadvantages of welding high-strength S700MC steel without preheating.

Figure 9
Tensile Test Results

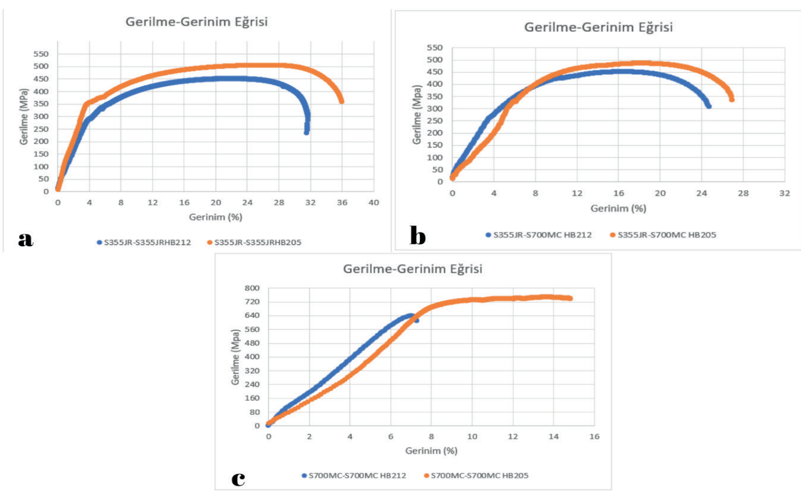

When examining the tensile test results of samples obtained from the source of S355JR structural steel under HB 205 mixed gas, the average yield strength was found to be 355 MPa, the tensile strength was 500 MPa, and the elongation (percentage elongation) was 36%. When examining the tensile test results of S355JR structural steel samples obtained from the same source under HB 212 mixed gas, the average yield strength was found to be 300 MPa, the tensile strength was 450 MPa, and the elongation (percentage elongation) was 31.5% **(Figure 9a)**. The S355JR steel exhibited performance above the percentage elongation values given in the material certificate. The yield stress, tensile stress, and strain values of the tensile bars welded with HB212 mixed gas were also low when compared to the samples welded with HB205 mixed gas, and consequently, a more brittle structure was observed. The high CO2 content in the HB212 mixture gas increased the hardness of the thin sheet metal structure, resulting in a more brittle material. The average yield strength of samples obtained from S355JR and S700MC structural steel welded with HB205 mixture gas was found to be 350 MPa, tensile strength 490 MPa, and elongation 27%. When looking at the values obtained from rods welded with HB212 mixed gas, they are relatively lower; the yield strength is 270 MPa, the tensile strength is 450 MPa, and the elongation is 24.7% **(Figure 9b)**.

It was observed that lower values were obtained when S700MC structural steel was welded with HB212 mixed gas, as was the case with other samples. The yield and tensile stresses and elongation values of the tensile bars welded with HB205 were 700 MPa, 740 MPa, and 15%, respectively, while those of the samples welded with HB212 were 610 MPa, 640 MPa, and 7.3% **(Figure 9c)**. Considering the requirements that the weld of the HB212 welded specimens must have a yield strength of 700 MPa, a tensile strength of 750-949 MPa, and a minimum elongation of 12%, as specified in the TS EN 10149-2 standard for S700MC steels, it was found that the weld was not suitable (Ulaştı, 2018). Although the test results of the specimens welded with HB205 fell within these values, their welds were found to be unsuitable due to fracture zones.

Conclusion

- It was observed that the chemical composition ratio of the gas used did not affect the grain size.
- It was observed that grain sizes increased in the HAZ and welded regions, and the equiaxed grain structure transformed into dendritic branches.
- Relatively lower hardness values were obtained in sample S1 compared to sample S4. Lower hardness values were obtained in sample S5 compared to sample S2.
- The hardness values of samples S3 and S6 are almost identical.
- It was observed that the hardness values of both metals in the HAZ and weld metal did not exceed the maximum hardness values required.
- Upon examining the XRD analysis results, it was determined that the most

intense fundamental peak in the phase analysis of all materials exhibited the iron (Fe) phase.

- In the XRD analysis, it can be stated that the microstructure of the main materials and welded joints consists of a ferrite phase.
- Although residual stresses are high after welding due to the high cooling rate caused by the thin material thickness, S355JR steel welded with HB205 mixed gas has good mechanical properties. The elongation and tensile strength meet the values specified in the material certificate. The high CO_2 content in the HB212 mixed gas resulted in a more brittle structure, reducing ductility.
- Although S700MC steel yielded better results in the HB205 mixed gas test, examination of the fracture zone revealed brittle fracture at the welded area. This demonstrates the necessity of heat treatment.
- Although the S355JR and S700MC combination has relatively better mechanical properties than the combination of S700MC steels, it has low mechanical properties. In the tensile test, the fracture occurred in the S355JR steel, which has a lower strength value.

References

Anık, S. (1991). *Kaynak tekniği el kitabı*. İstanbul: Gedik Eğitim Vakfı.

Ayyıldız, E. A. (2022). *Aşınmaya dirençli HBW450 Hardox çeliği ve S355J2 yapı çeliğinin robotik gazaltı kaynak yöntemi ile birleştirilmesi ve metalurjik özelliklerinin değerlendirilmesi* (Yüksek Lisans Tezi). Gazi Üniversitesi Fen Bilimleri Enstitüsü, Ankara.

Çetin, V. (2019). *Treyler şaselerinde kullanılan S700 MC çelik saclarının elektrik direnç nokta kaynağında mekanik özelliklerinin incelenmesi* (Yüksek Lisans Tezi). Sakarya Uygulamalı Bilimler Üniversitesi Lisansüstü Eğitim Enstitüsü, Sakarya.

ChnÇelik. (2023). Guide to citing Internet sources. Retrieved 24 December 2023, from https://www.chncelik.com.tr/teknik-dokumanlar/st-52-s355jr-celik-ozellikleri/

Demirci, D. (2010). *Muhtelif kaynak yöntemlerinde doğru akımlı kaynakta kutuplamanın kaynak dikiş formuna etkilerinin araştırılması* (Yüksek Lisans Tezi). Dokuz Eylül Üniversitesi Fen Bilimleri Enstitüsü, İzmir.

Dikeç, S. (2023). *Erdemir Test Sertifikası*. Kocaeli.

Durmuşoğlu, Ş. (2006). *Gazaltı kaynağında kaynak kalitesine tesir eden parametrelerin mekanik özelliklere etkisi* (Yüksek Lisans Tezi). Kocaeli Üniversitesi Fen Bilimleri Enstitüsü, Koaceli.

Ekinci, Ö., & Balalan, Z. (2019). Microhardness and microstructure of fiber laser welded S960 and S700 steels. *International Journal of Innovative Engineering Applications*, *3*, 15–21.

Eryürek, B., Sevük, A., & Odabaş, A. (2007). *Kaynak teknolojisi* (2nd ed.). İstanbul: Askaynak.

Eski, Ö. (2001). *Kaynak ısı girdisinin soğuk şekillendirilmiş S700MC çeliğinin mekanik özelliklerine etkisi* (Yüksek Lisans Tezi). İstanbul Teknik Üniversitesi Fen Bilimleri Enstitüsü, İstanbul.

Geçmen, İ. (2006). *Çeliklere gazaltı kaynağının uygulanması* (Yüksek Lisans Tezi). Marmara Üniversitesi Fen Bilimleri Enstitüsü, İstanbul.

Górka, J., & Stano, S. (2018). Microstructure and properties of hybrid laser arc welded joints (laser beam-MAG) in thermo-mechanical control processed S700MC steel. *Metals*, *8*(2). doi:10.3390/met8020132

Gür, Y. (2022). *MIG/MAG kaynağı ile birleştirilen S700 MC yüksek dayanımlı yapı çeliğinin mikroyapı ve mekanik özelliklerinin incelenmesi* (Yüksek Lisans Tezi). Gazi Üniversitesi Fen Bilimleri Enstitüsü, Ankara.

Karakoç, S. (2012). *Çeliklere gazaltı kaynağının uygulanması ve kaynağa etki eden parametreler* (Yüksek Lisans Tezi). Mustafa Kemal Üniversitesi Fen Bilimleri Enstitüsü, Hatay.

Kaya, Y., Çayırhan, G., Bökü, M., & Kahraman, N. (2020). Paslanmaz çelik ile düşük karbonlu çelik malzemelerin MIG kaynak yöntemiyle birleştirilebilirliğinin incelenmesi. *NWSA Academic Journals*, *15*(2), 89–99. doi:10.12739/nwsa.2020.15.2.1a0453

Koç, M. (2009). *Elektrik ark kaynağında kaynak gazı ve dumanının kaynak parametrelerine göre analizi* (Yüksek Lisans Tezi). Gazi Üniversitesi Fen Bilimleri Enstitüsü, Ankara.

Küpeli, G. (2008). *Alaşımsız çeliklere robotik gazaltı kaynağının uygulanması* (Yüksek Lisans Tezi). Marmara Üniversitesi Fen Bilimleri Enstitüsü, İstanbul.

Morrow Welding. (n.d.). Retrieved 2 September 2025, from https://www.morrowwelding.com/tr/news/classification-of-droplet-transition-in-gas-metal-arc-welding/

Özkan, E. (2019). *Kaynak sonrası S355J2N yapı çeliğinde oluşan gerilmeleri gidermek için uygulanan ısıl işlemin etkilerinin tahribatlı-tahribatsız muayene yöntemleriyle belirlenmesi* (Yüksek Lisans Tezi). Tekirdağ Namık Kemal Üniversitesi Fen Bilimleri Enstitüsü, Tekirdağ.

Şık, A. (2002). *Otomobil saclarının MIG/ MAG kaynağında gaz karışımlarının bağlantının mekanik özelliklerine etkisi* (Doktora Tezi). Gazi Üniversitesi Fen Bilimleri Enstitüsü, Ankara.

Şık, A. (2007). MIG/MAG kaynağı ile kaynatılan çelik yapılarda koruyucu gaz karışımlarının mekanik özelliklere etkilerinin araştırılması*. *Tujs Trakya Univ J*

Sci, *8*(1), 55–60. Retrieved from http://fbe.trakya.edu.tr/

Stephanie Oostman. (2021). GMAW Equipment and Setup. In *Introduction to Welding* (pp. 418–433). Washington: Washington Open Proftech.

Toprak Şenol, H. (2020). *Zeki sistemler ile ark kaynağı elektrotlarındaki kaynak parametrelerinin incelenmesi* (Yüksek Lisans Tezi). Muğla Sıtkı Koçman Üniversitesi Fen Bilimleri Enstitüsü, Muğla.

Tukahirwa, G., & Wandera, C. (2023). Influence of Process Parameters in Gas-Metal Arc Welding (GMAW) of Carbon Steels. In *Welding - Materials, Fabrication Processes, and Industry 5.0*. IntechOpen. doi:10.5772/intechopen.1002730

Ulaştı, E. (2018). *Termomekanik haddeleme ile S700MC kalite çeliklerin üretimi ve üretim parametrelerinin mekanik özelliklere etkisinin incelenmesi* (Yüksek Lisans Tezi). İstanbul Teknik Üniversitesi Fen Bilimleri Enstitüsü, İstanbul.

About The Authors

Fatma Nur ŞAHİN, MSc, graduated from Necmettin Erbakan University, Institute of Science, Department of Mechanical Engineering. She is a PhD student at Necmettin Erbakan University and worked as a quality and production manager in the forklift and trailer industry. She is worked in the supervision and management of welded manufacturing applications, which is her main area of expertise.

E-mail: fnursahin7@gmail.com **ORCID:** 0000-0001-6071-0168

Hakan GÖKMEŞE, PhD, is a Professor of Mechanical Engineering at Necmettin Erbakan University in Konya, Turkey. I have a master's degree in Metallurgical Education from Gazi University. His main areas of interest are casting technology, powder metallurgy, heat treatments, and composites and nanocomposites applications.

E-mail: hakan1440@gmail.com, **ORCID:** 0000-0003-0053-8444

Şaban BÜLBÜL, PhD, is an Associate Professor of Mechanical Engineering at Necmettin Erbakan University in Konya, Turkey. I have a master's degree in Metalurgical Education from Karabuk University. His main areas of interest are casting technology, powder metallurgy, polymer materials, and polymer applications.

E-mail: sabanbulbul42@hotmail.com , **ORCID:** 0000-0002-9268-1469

Similarity Index

The similarity index obtained from the plagiarism software for this book chapter is 10 %.